

Fig. 10. L_1 vs $H_2 - n$'s diagonal elements

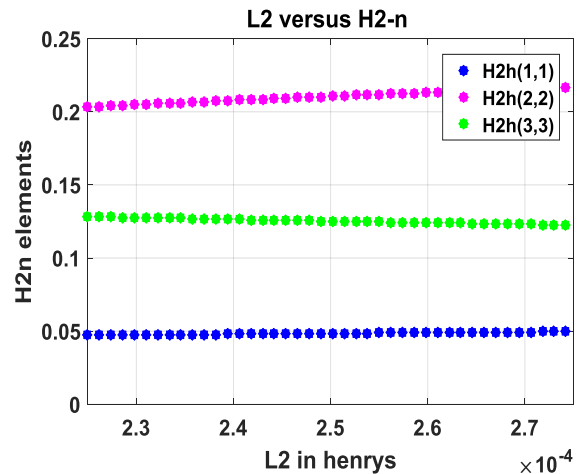


Fig. 13. L_2 vs $H_2 - n$'s diagonal elements.

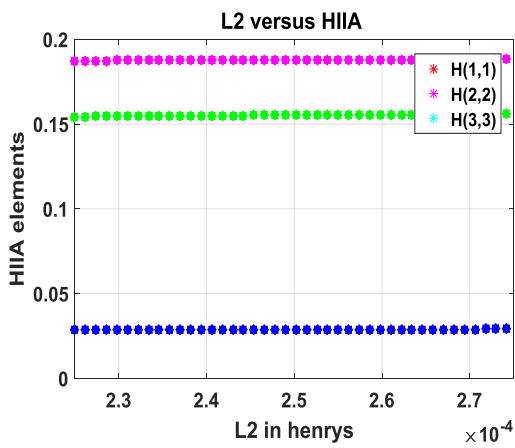


Fig. 11. L_2 vs $HIIA$'s diagonal elements

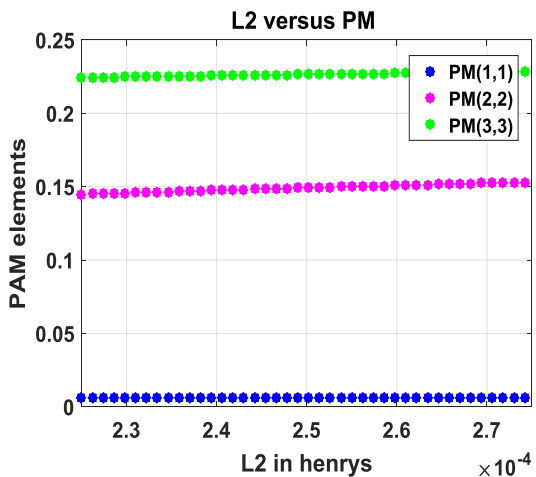


Fig. 12. L_2 vs PM 's diagonal elements.

5.4. L_3 variation in relation to interaction matrix elements:

L_3 variation, which is varied by $\pm 20\%$, is taken into consideration to examine how it affects interactions. In Figs. 14-16, the effects of each parameter on the interaction measures are visually displayed.

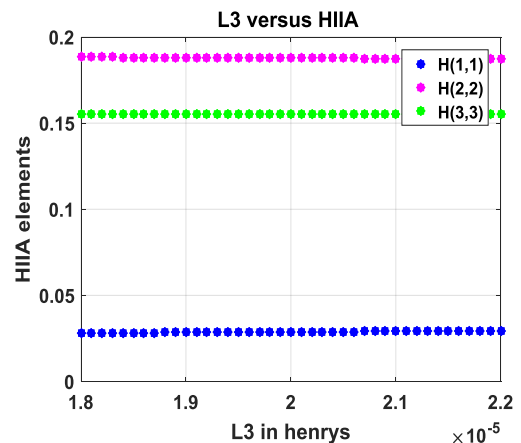


Fig. 14. L_3 vs $HIIA$'s diagonal elements.

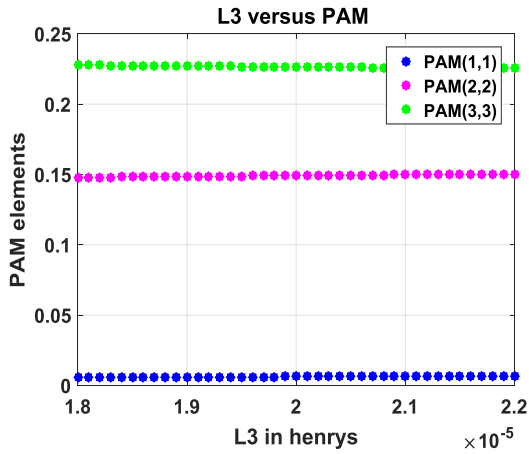


Fig. 15. L_3 vs PM 's diagonal elements.

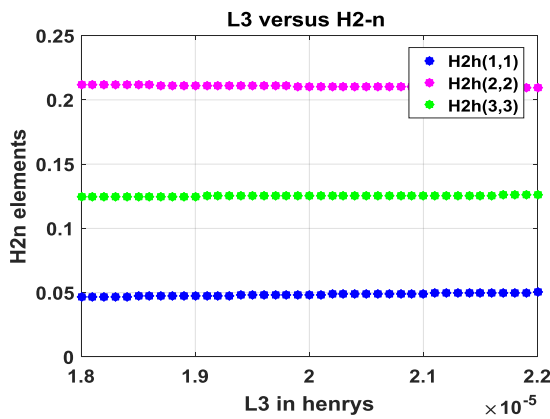


Fig. 16. L_3 vs $H_2 - n$'s diagonal elements.

Fig. 17. C_o vs $HIIA$'s diagonal elements.

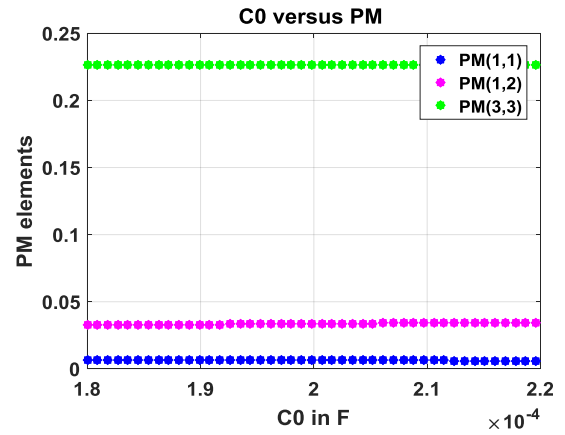


Fig. 18. C_o vs PM 's diagonal elements.

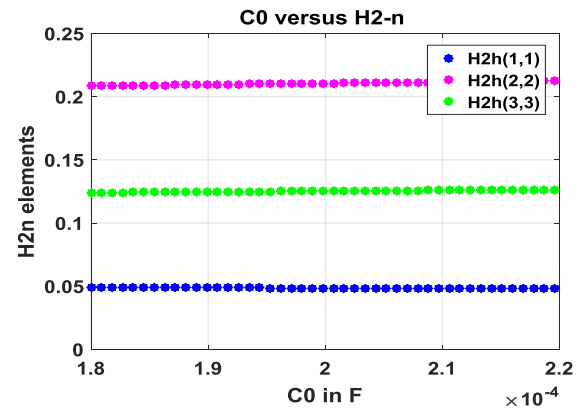
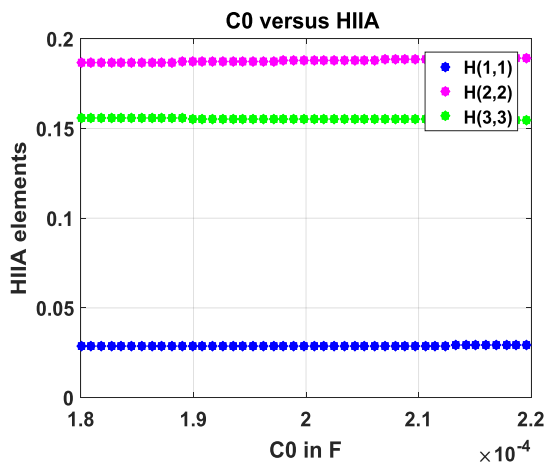


Fig. 19. C_o vs $H_2 - n$'s diagonal elements.

5.5. C_o variation in relation to interaction matrix elements:

C_o variation, which is varied by $\pm 20\%$, is taken into consideration to examine how it affects interactions. In Figs. 17-19, the effects of each parameter on the interaction measures are visually displayed.



6. Simulations and Experimental Results

Figure 20 shows the test bench, and using RT-LAB simulation software, the accuracy of the TIID converter is verified in the MATLAB environment that is connected to the OPAL4510-RT simulator. OPAL4510-RT is the name of the Hardware-in-the-Loop (HIL) testing device [24],[25]. An oscilloscope is utilized for real-time observations for digital storage (DSO) and is used to simulate the converter.

The simulated outputs V_o , I_o and duty ratios d_1, d_2 and d_3 under nominal operating conditions given in Table A1 are shown in Figs. 21 and 22 respectively. The corresponding OP4510 HIL Simulation results measured in DSO are shown in Figs. 23-25, respectively.

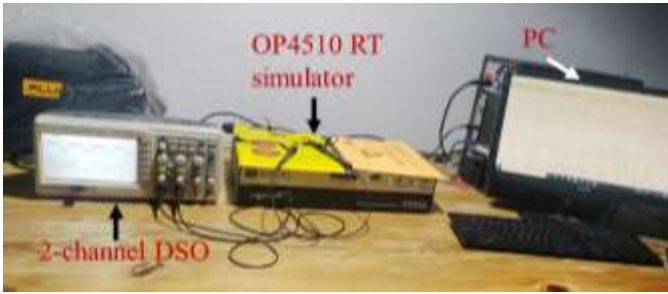


Fig. 20. OPAL4510-RT Simulator test bench

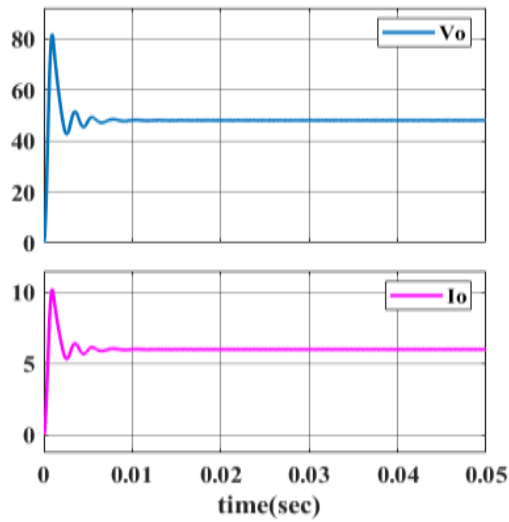


Fig.21. TIID converter's V_o , I_o

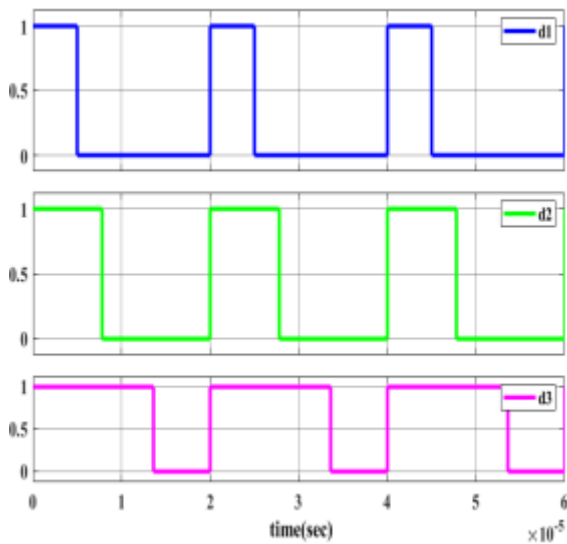


Fig.22. duty ratios of the converter

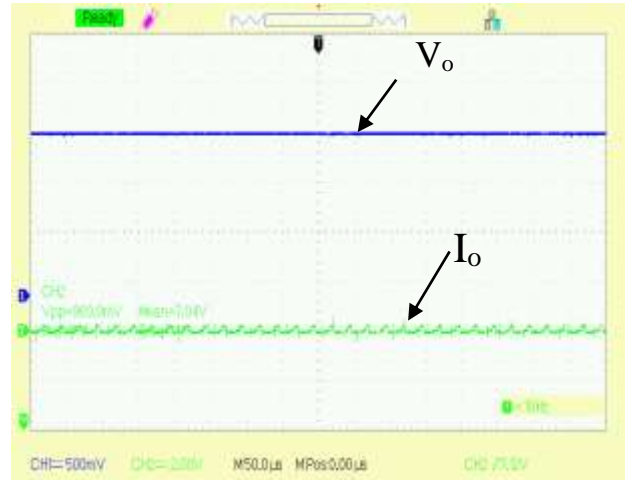


Fig.23. V_o , I_o of TIID converter

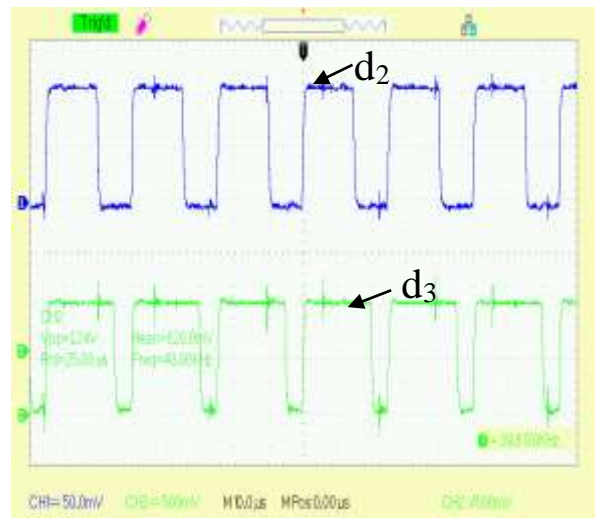


Fig.24. duty ratios d_2 , d_3 of TIID converter

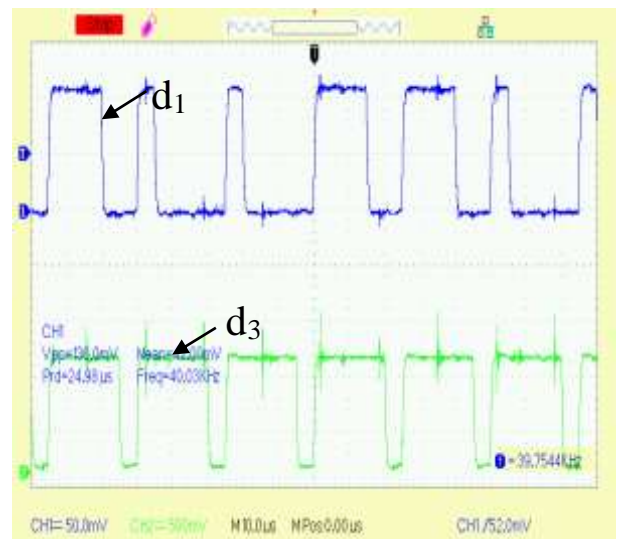


Fig.25. duty ratios d_1 , d_3 of TIID converter

7. Conclusion

The Frequency based (Gramian) interaction metrics ($H_2 - n$, H_{IIA} and PM) for a Three-Input Integrated Dc-Dc (TIID) converter were investigated and analysed. Methodologies and computational procedures are discussed. An analysis of the TIID converter's interaction measures is done using MATLAB programming. The analysis of the I/O pairing proposals offered by each measure shows that they all provide the same type of I/O pairing, which is diagonal pairing. It was found that the pairing ideas were always the same as the nominal suggestions after witnessing the interactions under different operating conditions. Plots are used to illustrate the effects of parameter changes on interaction measures. The results demonstrate that changes in the parameters have no effect on the interaction measurements. The experimental findings of the TIID converter are obtained using the Hardware In Loop (HIL) environment of the OPAL RT simulator OP4510 integrated with MALTAB.

The future scope of this work is (i) to design different diagonal controllers for TIID converter as suggested by Gramian measures, (ii) to analyse the stability of all the designed closed-loop TIID converter systems, (iii) the sensitivity analysis is to be carried out.

APPENDIX

The TIID converter operates on a 48V dc-bus regulation. Table A1 lists the specifications that are taken into consideration here. With these parameters, MATLAB calculates the TFM G of the TIID converter taking into account every mode described in section 2 and provides G as given in (5) from (A1)- (A9).

Table A1: Specifications and Parameter Values

Parameters	Value
V_{g1}, V_{g2}, V_{g3}	36V,30V,24V
V_o , Load power P_o	48V, 288W
i_{L1}, i_{L2}	2.5A,2A
L_1, L_2, L_3	150μH,250μH, 20μH

C_o	200μF
Switching frequency f_s	50KHz
$\Delta i_L, \Delta V_o$	10%, 5%

$$G_{11} = \frac{-0.3488s^4 - 2.493x10^4s^3 + 1.051x10^9s^2 + 5.608x10^{12}s + 1.796x10^{15}}{s^4 + 6195s^3 + 6.126x10^7s^2 + 1.3x10^{11}s + 2.885x10^{13}} \quad (A1)$$

$$G_{12} = \frac{0.6379s^4 + 1.293x10^5s^3 + 6.573x10^9s^2 + 2.308x10^{12}s + 6.963x10^{13}}{s^4 + 6195s^3 + 6.126x10^7s^2 + 1.3x10^{11}s + 2.885x10^{13}} \quad (A2)$$

$$G_{13} = \frac{-0.4423s^4 - 4.073x10^4s^3 + 3.755x10^8s^2 + 2.48x10^{12}s + 8.226x10^{13}}{s^4 + 6195s^3 + 6.126x10^7s^2 + 1.3x10^{11}s + 2.885x10^{13}} \quad (A3)$$

$$G_{21} = \frac{3.249x10^5s^3 + 2.093x10^9s^2 + 1.442x10^{13}s + 1.382x10^{16}}{s^4 + 6195s^3 + 6.126x10^7s^2 + 1.3x10^{11}s + 2.885x10^{13}} \quad (A4)$$

$$G_{22} = \frac{-4253s^3 - 7.506x10^8s^2 - 3.238x10^{13}s - 1.029x10^{16}}{s^4 + 6195s^3 + 6.126x10^7s^2 + 1.3x10^{11}s + 2.885x10^{13}} \quad (A5)$$

$$G_{23} = \frac{2949s^3 + 1.943x10^8s^2 - 1.899x10^{12}s - 1.215x10^{16}}{s^4 + 6195s^3 + 6.126x10^7s^2 + 1.3x10^{11}s + 2.885x10^{13}} \quad (A6)$$

$$G_{31} = \frac{4.446x10^7s^2 - 2.665x10^{12}s - 1.243x10^{16}}{s^4 + 6195s^3 + 6.126x10^7s^2 + 1.3x10^{11}s + 2.885x10^{13}} \quad (A7)$$

$$G_{32} = \frac{-2552s^3 - 4.15x10^8s^2 - 1.577x10^{13}s - 1.4x10^{15}}{s^4 + 6195s^3 + 6.126x10^7s^2 + 1.3x10^{11}s + 2.885x10^{13}} \quad (A8)$$

$$G_{33} = \frac{1.967x10^5s^3 + 1.237x10^9s^2 + 1.061x10^{13}s + 1.592x10^{16}}{s^4 + 6195s^3 + 6.126x10^7s^2 + 1.3x10^{11}s + 2.885x10^{13}} \quad (A9)$$

References

- [1] H. Matsuo, W. Lin, F. Kurokawa, T. Shigemizu, and N. Watanabe, "Characteristics of the multiple-input DC-DC converter," *IEEE Trans. Ind. Electron.*, vol. 51, no. 3, pp. 625-631, Jun. 2004.

- [2] J. Zhou, G. Nygaard and E. H. Vefring, "Adaptive decentralized control of DC-DC converter systems," 2012 7th IEEE Conference on Industrial Electronics and Applications (ICIEA), 2012, pp. 576-581.
- [3] S. Skogestad and I. Postlethwaite, "Multivariable Feedback Control: Analysis and Design," John Wiley & Sons, 1996.
- [4] D. Chen and D. E. Seborg, "Relative gain array analysis for uncertain process models," *AIChE journal*, Vol. 48 no. 2, pp. 302-310, Feb. 2002.
- [5] Conley and M. E. Salgado, "Gramian based interaction measure," in Proc. of *IEEE Int. Conference, CDC 2000*, vol. 5, pp. 5020-5022.
- [6] B. Wittenmark and M. E. Salgado, "Hankel-norm based interaction measure for input-output pairing," *IFAC World Congress*, vol. 139, pp. 429-434, Jan. 2002.
- [7] Yuan-Chuan Liu and Yaow-Ming Chen, "A Systematic Approach to Synthesizing Multi-Input DC-DC Converters," *IEEE transactions on power electronics*, vol. 24, no. 1, January 2009, pp. 116-127.
- [8] B. A. Reddy and M. Veerachary, "Gramian based digital controller design for two-input integrated DC-DC converter," *2013 International Conference on Control Communication and Computing (ICCC)*, 2013, pp. 335-340, doi: 10.1109/ICCC.2013.6731675
- [9] B. A. Reddy and M. Veerachary, "Hankel-norm based interaction analysis and digital controller design for two-input integrated DC-DC converter," *2013 Annual IEEE India Conference (INDICON)*, 2013, pp. 1-6, doi: 10.1109/INDCON.2013.6725943
- [10] P. Thota, A. R. Bhimavarapu and V V S Bhaskara Reddy Chintapalli, "Selection of input-output pairing and control structure configuration using interaction measures for DC-DC dual input zeta-SEPIC converter," *Electrica.*, November 12, 2022.
- [11] Thota, P., Bhimavarapu, A.R. and Chintapalli, V.V.S.B.R. (2022), "Participation Factor based analysis of PVSC type Multi-Input Zeta-SEPIC dc-dc converter", *COMPEL - The international journal for computation and mathematics in electrical and electronic engineering*, Vol. 41 No. 5, pp. 1727-1752. <https://doi.org/10.1108/COMPEL-10-2021-0363>
- [12] S. Upadhyaya and M. Veerachary, "Interaction Quantification in Multi-Input Multi-Output Integrated DC-DC Converters," *2021 IEEE 4th International Conference on Computing, Power and Communication Technologies (GUCON)*, 2021, pp. 1-6, doi: 10.1109/GUCON50781.2021.9573935.
- [13] Ling-Jian Ye and Zhi-huan Song, "New loop pairing criterion based on interaction and integrity considerations", *Journal of Zhejiang University: Science C* 11(5):381-393, May 2010.
- [14] Fredrik Bengtsson, Torsten Wik, "Finding feedforward configurations using gramian based interaction measures", *Modeling, Identification and Control*, Vol. 42, No. 1, 2021, pp. 27-35, ISSN 1890-1328.
- [15] Guo, X.; Shirkhani, M.; Ahmed, E.M, "Machine-Learning-Based Improved Smith Predictive Control for MIMO Processes", *Mathematics* **2022**, 10, 3696. <https://doi.org/10.3390/math10193696>.
- [16] Sumit Kumar Pandey, Jayati Dey, Subrata Banerjee, "Generalized discrete decoupling and control of MIMO systems", *Asian Journal of Control*, Volume 24, Issue 6, November 2022, Pages 3326-3344.
- [17] A. Gupta, R. Ayyanar and S. Chakraborty, "Novel Electric Vehicle Traction Architecture With 48 V Battery and Multi-Input, High Conversion Ratio Converter for High and Variable DC-Link Voltage," in *IEEE Open Journal of Vehicular Technology*, vol. 2, pp. 448-470, 2021, doi: 10.1109/OJVT.2021.3132281.
- [18] I. Alhamrouni, M. Salem, Y. Zahraoui, B. Ismail, A. Jusoh, and T. Sutikno, "Multi-input interleaved DC-DC converter for hybrid renewable energy applications," *Bulletin of Electrical Engineering and Informatics*, vol. 11, no. 3, pp. 1765-1778, Jun. 2022, doi: 10.11591/eei.v11i3.3779.
- [19] B. R. Ravada, N. R. Tummuru and B. N. L. Ande, "Photovoltaic-Wind and Hybrid Energy Storage Integrated Multi-Source Converter Configuration for DC Microgrid Applications," in *IEEE Transactions on Sustainable Energy*, vol. 12, no. 1, pp. 83-91.

- [20] V. Häberle, M. W. Fisher, E. Prieto-Araujo and F. Dörfler, "Control Design of Dynamic Virtual Power Plants: An Adaptive Divide-and-Conquer Approach," in *IEEE Transactions on Power Systems*, vol. 37, no. 5, pp. 4040-4053, Sept. 2022, doi: 10.1109/TPWRS.2021.3139775.
- [21] E. Sánchez-Sánchez, D. Groß, E. Prieto-Araujo, F. Dörfler and O. Gomis-Bellmunt, "Optimal Multivariable MMC Energy-Based Control for DC Voltage Regulation in HVDC Applications," in *IEEE Transactions on Power Delivery*, vol. 35, no. 2, pp. 999-1009, April 2020, doi: 10.1109/TPWRD.2019.2933771.
- [22] A. Khodamoradi, G. Liu and P. Mattavelli, "Online Controller Tuning for DC Microgrid Power Converters With the Ability to Track Maximum Allowable Bandwidth," in *IEEE Transactions on Industrial Electronics*, vol. 69, no. 2, pp. 1888-1897, Feb. 2022, doi: 10.1109/TIE.2021.3057009.
- [23] M. Manogna, B. A. Reddy and K. Padma, "Modeling of a Three-Input Fourth-Order Integrated DC-DC Converter," *2022 International Conference on Smart and Sustainable Technologies in Energy and Power Sectors (SSTEPS)*, Mahendragarh, India, 2022, pp. 83-88, doi: 10.1109/SSTEPS57475.2022.00032.
- [24] Santosh Kumar Reddy, P.L., Obulesu, Y.P. Design and Development of a New Transformerless Multi-port DC-DC Boost Converter. *J. Electr. Eng. Technol.* (2022). <https://doi.org/10.1007/s42835-022-01145-9>.
- [25] Anjali Atul Bhandakkar and Lini Mathew Dr. 2018 IOP Conf. Ser.: Mater. Sci. Eng. 331 012028.